

Black hole shadow, photon ring and lensing ring in the CDM halo

Shi-Jie Ma, Tian-Chi Ma, Jian-Bo Deng, and Xian-Ru Hu*

Lanzhou Center for Theoretical Physics,

Key Laboratory of Theoretical Physics of Gansu Province,

Lanzhou University, Lanzhou, Gansu 730000, China

(Dated: June 28, 2022)

arXiv:2206.12820v1 [gr-qc] 26 Jun 2022

Abstract

In this paper, the Schwarzschild black hole in the CDM halo is deeply studied, and the radiation laws of the thin accretion disk near the black hole is discussed and summarized. Firstly, the physical concepts involved in this paper are briefly introduced in the first chapter. In the following chapters, the light orbits around the black hole are calculated. According to the number of times that the light from the north pole passes through the equatorial plane of the black hole, the light orbits can be divided into three categories: direct orbit, lensed orbit and photon ring orbit. At the same time, the innermost stable circular orbit of the black hole is also calculated. Finally, by analyzing the calculation results of radiation intensity of three kinds of radiation which emitted by thin accretion disk on the equatorial plane of black hole and observed at infinity away from the north pole of black hole, the radiation laws of the thin accretion disk of Schwarzschild black hole suitable for the background of the CDM halo is summarized. Finally, the follow-up work is prospected.

keywords: the CDM halo, spherically symmetric black hole; accretion disk, null geodesic.

* huxianru@lzu.edu.cn

I. INTRODUCTION

Since Einstein established general relativity, general relativity has explained and predicted many phenomena in cosmic research, and cosmology has made new development [1–4]. However, in the process of development in recent years, there has been a gravitational effect that cannot be explained unless there is more invisible matter. To solve this problem, cosmologists proposed the existence of dark matter. It is now generally believed that dark matter accounts for about 85 % of the universe [5–7]. It does not seem to interact with electromagnetic fields, which means that it does not absorb, reflect or emit electromagnetic radiation, so it is difficult to be observed. Due to the gravitational effect that cannot be explained by the existing gravitational theory, dark matter should have gravitational effect with ordinary matter.

James Peebles first proposed the cold dark matter(CDM) model in [8]. Cold means that dark matter moves slowly relative to the speed of light. The prediction of the CDM paradigm is basically consistent with the observation of large-scale structure of cosmology. Since the late 1980s or 1990s, most cosmologists tend to use the CDM theory (especially the Λ CDM model [9, 10]) to describe how the universe developed from the early smooth initial state to the massive distribution of galaxies and star clusters we see today.

According to the model of modern physical cosmology, dark matter halo is the basic unit of cosmic structure. The hypothesis for CDM structure formation begins with

density perturbations in the Universe that grow linearly until they reach a critical density, after which they would stop expanding and collapse to form gravitationally bound dark matter halos [11].

In [12], the author clearly gives the metric of the CDM halo. This provides theoretical help for us to study the spherically symmetric black hole in the CDM halo.

As we know, a shadow is a darker area formed when an opaque object blocks the transmission of light. By definition, the shape of a shadow depends on the location and intensity of the light source. The same is true of black hole shadows. For the standard use of the term "shadow", light sources are considered to be scattered throughout the space, including from behind the observer. However, if a specific light source near the black hole is so bright (the thin accretion disk is relatively bright and has thermomagnetic spectrum [13, 14], this paper takes the thin accretion disk as the specific light source) that the natural light source can be ignored, the appearance of the black hole cannot be described by the standard "shadow". To avoid ambiguity, we refer to the standard "shadow" as the "critical curve" suggested in [15]. The size of the observed central dark area is mainly controlled by the emission profile and gravitational redshift, so there is more physical information in the so-called photon ring and lensing ring [15–19].

In order to more fully understand the appearance of black holes in the CDM

halo, we will take the Schwarzschild black hole in the CDM halo as an example to conduct a comprehensive analysis of shadows, photon rings and lensing rings. In Section II, the null geodesic of Schwarzschild black hole in the CDM halo is calculated. In Section III, we classify it according to its orbit deflection angle and analyze the relationship between the halo radius and the parameters of the CDM halo. In Section IV, we calculate the relationship between the light intensity emitted by the thin accretion disk and the observed light intensity of the viewer and the transfer function. In Section V, three typical radiation models are selected for calculation, and the laws applicable to any radiation in the CDM halo are summarized. We give a conclusion and outlook in Section VI. In this paper, in order to simplify the calculation, $G_N = M = C = 1$.

II. NULL GEODESIC IN THE CDM HALO

In [12], we get the metric of Schwarzschild black hole in the CDM halo.

$$ds^2 = g_{\mu\nu} dx^\mu dx^\nu = -g(r) dt^2 + \frac{dr^2}{g(r)} + r^2 (d\theta^2 + \sin^2 \theta d\varphi^2), \quad (1)$$

where

$$g(r) = \left(1 + \frac{r}{R_0}\right)^{-\frac{8\pi\rho_0 R_0^3}{r}} - \frac{2}{r}. \quad (2)$$

ρ_0 is the density of the CDM halo collapse, R_0 is the feature radius. It can be seen that when $\rho_0 = 0$ or $R_0 \rightarrow 0$, $g(r)$ will degenerate to $1 - 2/r$, so the gauge will

degenerate to Schwarzschild gauge.

The null geodesic($d^2s = 0$) equation under any metric is

$$\frac{d^2x^\sigma}{d\lambda^2} + \Gamma_{\mu\nu}^\sigma \frac{dx^\mu}{d\lambda} \frac{dx^\nu}{d\lambda} = 0, \quad (3)$$

where $\Gamma_{\mu\nu}^\sigma$ are Christoffel symbols, they are given by

$$\Gamma_{\mu\nu}^\sigma = \frac{1}{2}g^{\sigma\delta} (\partial_\mu g_{\delta\nu} + \partial_\nu g_{\mu\delta} - \partial_\delta g_{\mu\nu}) \quad (4)$$

For the static spherically symmetric metric, we can always limit the motion of particles on the equatorial plane, that is $\theta = \pi/2$ and $d\theta/ds = 0$, so we can get the following three equations:

$$\frac{dt}{ds} = \frac{E}{g(r)}, \quad (5)$$

$$\frac{d\varphi}{ds} = \frac{L}{r^2}, \quad (6)$$

$$\left(\frac{dr}{ds}\right)^2 = E^2 - g(r) \frac{L^2}{r^2}, \quad (7)$$

where E is energy and L is angular momentum, both of which are conserved quantities. Eliminate the affine parameter to get

$$\left(\frac{dr}{d\varphi}\right)^2 = r^4 \left(\frac{1}{b^2} - \frac{g(r^2)}{r^2}\right) = V_{eff} \quad (8)$$

where $b = L/E$ is called the impact parameter.

In addition to the circular orbit of light, we also need to know the relationship between all the trajectories of light and b . For simple calculation, replace r with

$u = 1/r$. The orbital equation becomes

$$\left(\frac{du}{d\varphi}\right)^2 = G(u), \quad (9)$$

where

$$G(u) = \frac{1}{b^2} - u^2 \left(\left(1 + \frac{1}{uR_0}\right)^{-8\pi\rho_0 R_0^3 u} - 2u \right). \quad (10)$$

According to Eq. (9) and Eq. (10), we calculate that the total variation of light orbit azimuth of any b is

$$\varphi = \begin{cases} 2 \int_0^{u_m} \frac{du}{\sqrt{G(u)}} du & b > b_c \\ \int_0^{u_0} \frac{du}{\sqrt{G(u)}} du & b < b_c \end{cases}, \quad (11)$$

which b_c is the impact parameter corresponding to the circular orbit of light (i.e. photon sphere), we can get b_c and corresponding radius r_c by $V_{eff} = V'_{eff} = 0$. At $b > b_c$, light will not fall into the black hole; at $b < b_c$, light will fall into the black hole. u_m is the turning point at $b > b_c$, corresponding to the minimum positive real root of $G(u) = 0$, and $u_0 = 1/r_0$.

III. DIRET, LENSING AND PHOTON RING IN THE CDM HALO

In Section II, we calculated the bending of light near the black hole, in this section, we will classify according to the bending angle of light. In order to discuss the observation of light emission near a black hole, according to the number of times

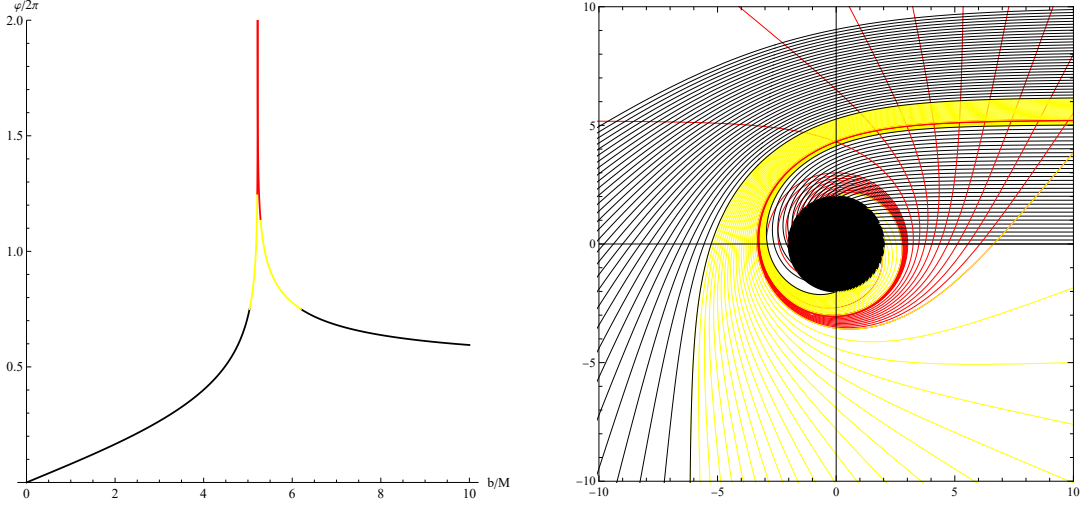


Figure 1: The relationship between φ and b (left) and the orbit of light near the black hole in the CDM halo(right). We set $\rho_0 = 0.1$, $R_0 = 0.1$. Different colors correspond to $\varphi < 3\pi/2$ (black), $3\pi/4 < \varphi < 5\pi/4$ (yellow) and $\varphi > 5\pi/4$ (red), which are defined as direct, lensing and photon ring orbits respectively. On the right, we show the Euclidean polar coordinates (r, φ) . The relevant photon orbits in are the direct orbit (black), lensing orbit (yellow) and photon ring orbit (red) bands. The black hole is shown as a black disk in the middle of the image.

m that the light emitted at infinity in the north pole of the black hole passes through the equatorial plane of the black hole, we divide the light emission orbit into direct orbit($m = 1$), lensing orbit($m = 2$) and photon ring orbit($m = 3$). We define $b_m^- < b_c$

Table I: Various important physical parameters when $\rho_0 = 0.1$ and R_0 takes different values.

R_0	r_0	r_c	b_1^-	b_2^-	b_3^-	b_c	b_3^+	b_2^+
0	2	3	2.8477	5.0151	5.1878	5.1962	5.2279	6.1678
0.1	2.0076	3.0117	2.8588	5.0363	5.2102	5.2156	5.2834	6.1965
0.2	2.0481	3.0740	2.9181	5.1515	5.3321	5.3409	5.4675	6.3575
0.3	2.1375	3.2125	3.0498	5.4125	5.6096	5.6197	5.6574	6.7322

Table II: Various important physical parameters when $R_0 = 0.1$ and ρ_0 takes different values.

ρ_0	r_0	r_c	b_1^-	b_2^-	b_3^-	b_c	b_3^+	b_2^+
0	2	3	2.8477	5.0151	5.1878	5.1962	5.2279	6.1678
0.1	2.0076	3.0117	2.8588	5.0363	5.2102	5.2156	5.2834	6.1965
0.2	2.0153	3.0234	2.8700	5.0575	5.2325	5.2409	5.2733	6.2254
0.3	2.0229	3.0351	2.8811	5.0787	5.2548	5.2634	5.2733	6.2254

and $b_m^+ > b_c$. We use b_m^\pm represents the solution of the following equation.

$$\varphi(b) = \left(m - \frac{1}{2}\right) \pi, \quad m = 1, 2, 3 \dots \quad (12)$$

The physical picture of this classification is clear from the orbit plots in Fig. 1.

Assuming that the light is emitted from the north pole (the rightmost side of the orbit). When $b \rightarrow \infty$, the azimuth of light around the black hole changes to $\varphi \rightarrow \pi/2$, so there is no corresponding b_1^+ .

We tried to calculate r_0 , r_c , b_c , b_1^- , b_2^\pm and b_3^\pm for different ρ_0 and R_0 , and wrote them in Table I and Table II.

Table I shows various important physical parameters when $\rho_0 = 0.1$ and R_0 takes different values. Table II shows various important physical parameters when $R_0 = 0.1$ and ρ_0 takes different values.

From Table I we can know all parameters increase with the increase of R_0 , when ρ_0 without change. We can also know all parameters increase with the increase of ρ_0 , when R_0 without change from Table II. This means that the light from different regions observed by us will be farther away from the center of the black hole with the increase of ρ_0 and R_0 . However, comparing Table I and Table II, it can be found that R_0 has a greater impact on various parameters than ρ_0 . It can also be known from Table I and Table II that when $\rho_0 = 0$ and $R_0 \rightarrow 0$, the black hole degenerates to Schwarzschild black hole in vacuum, the parameters of the black hole will reach the minimum.

IV. OBSERVED SPECIFIC INTENSITIES AND TRANSFER FUNCTIONS

In general, the term "shadow" describes how a black hole is illuminated from all directions. In sections II and III, we have known the optical orbit near the black hole in the CDM halo. Now we are ready to consider a thin accretion disk on the equatorial plane around the black hole in the CDM halo. For the observer at infinity, the observed is more important than the light intensity distribution.

Now we consider a simple example, the radiation intensity of a thin accretion disk near a black hole depends only on the radial coordinates, and we do not consider the absorption of light. We assume that the disk is isotropic within the stationary frame of the stationary world line (i.e. the object is stationary). The following example is only used as a model to illustrate the gravitational lensing effect and gravitational redshift effect. We place the disk on the equatorial plane and the observer is in the North Pole. We use $I_\nu^{em}(r)$ to express the specific intensity of emission. ν is the transmission frequency in the stationary coordinate system. The relative intensity of the light that an observer at infinity will receive is $I_{\nu'}^{obs}$, ν' is the frequency observed by the observer at infinity of the stationary reference system, and the frequency redshift is caused by the gravitational effect $\nu' = \sqrt{g(r)}\nu$ [20]. Considering that there is a conserved quantity I_ν/ν^3 for a light [21], we can get

$$\frac{I_{\nu'}^{obs}}{\nu'^3} = \frac{I_\nu^{em}}{\nu^3}, \quad (13)$$

so the relative intensity we observed is

$$I_{\nu'}^{obs} = g^{3/2}(r) I_{\nu}^{em}(r). \quad (14)$$

The total intensity observed is an integral of all frequencies

$$I^{obs} = \int I_{\nu'}^{obs} d\nu' = \int g^2(r) I_{\nu}^{em} d\nu = g^2(r) I^{em}(r), \quad (15)$$

where $I^{em} = \int I_{\nu}^{em} d\nu$ is the total emission intensity at the accretion disk at r .

Due to the high intensity of the light emitted from the accretion disk, other light sources in the environment can be ignored. If a beam of light from the observer intersects with the emission disk, it means that the intersection point as a light source will contribute the observation brightness to the observer. As mentioned in Section II, a light may pass through the equatorial plane of the black hole many times, and these intersections will all become light sources, providing light intensity for the one orbit. Therefore, the observed intensity is the sum of the intensities of each intersection

$$I^{obs}(b) = \sum_m g^2(r) I^{em}|_{r=r_m(b)}, \quad (16)$$

where $r_m(b)$ is the so-called transfer function, which represents the radial position of the m -th intersection and the transmitting disk, that is, the radial coordinates of the luminous point. It should be emphasized that the absorption and reflection of light by the accretion disk and the loss of light intensity in the environment are not considered in our process, which is only an ideal model.

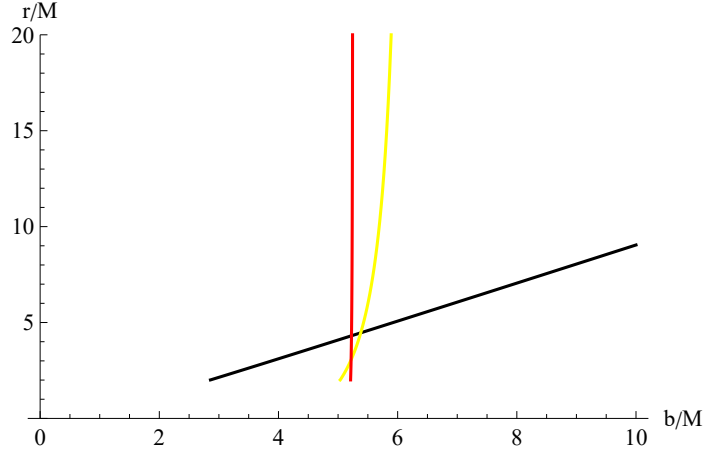


Figure 2: The first three transfer functions of black holes in the CDM halo with $\rho_0 = 0.1$, $R_0 = 0.1$. The three curves in the figure represent the radial coordinates of the first (black), second (yellow) and third (red) intersections with the accretion disk.

We denote the solution of orbit Eq. (14) by $u(b, \varphi)$, so we can get the transfer functions:

$$r_m(b) = \frac{1}{u\left(b, \frac{(2m-1)\pi}{2}\right)} \quad b \in (b_m^-, b_m^+), \quad (17)$$

here we take b_1^+ as positive infinity

V. RADIATION FROM STABLE CIRCULAR ORBIT

In Section IV, we calculate the relationship between the specific light intensity observed by the observer at infinity and the specific light intensity emitted by the

accretion disk, and calculate the relevant transfer function. As an example, the following typical model functions are employed to discuss the observed specific intensity. Firstly, we consider the emission is sharply peaked at the innermost stable circular orbit, and it ends abruptly at $r = r_{isco}$, such as

$$I^{em}(r) = \begin{cases} I^0 \frac{1}{(r-(r_{isco}-1))^2} & r \geq r_{isco} \\ 0 & r < r_{isco} \end{cases}. \quad (18)$$

ISCO is the innermost stable circular orbit of physical particles around a black hole($d^2 = -1$). V_{eff} in Eq. (7) becomes

$$V_{eff} = r^4 \left(\frac{E^2}{L^2} - \frac{g(r)}{L^2} - \frac{g(r)}{r^2} \right), \quad (19)$$

and the ISCO should satisfy $V_{eff} = V'_{eff} = V''_{eff} = 0$. So we can get r_{isco} by

$$\frac{\left(\frac{g(r_{isco})}{r_{isco}^2} \right)'}{g'(r_{isco})} = \frac{\left(\frac{g_{isco}}{r_{isco}^2} \right)''}{g''(r_{isco})}. \quad (20)$$

Secondly, we consider the emission is sharply peaked at the photon sphere, and it ends abruptly at $r = r_c$, such as

$$I^{em}(r) = \begin{cases} I^0 \frac{1}{(r-(r_c-1))^3} & r \geq r_c \\ 0 & r < r_c \end{cases}. \quad (21)$$

Finally, we consider a emission decaying gradually from the horizon, which is

$$I^{em}(r) = \begin{cases} I^0 \frac{1-\tanh(r-4.5)}{1-\tanh(r_0-4.5)} & r \geq r_0 \\ 0 & r < r_0 \end{cases}. \quad (22)$$

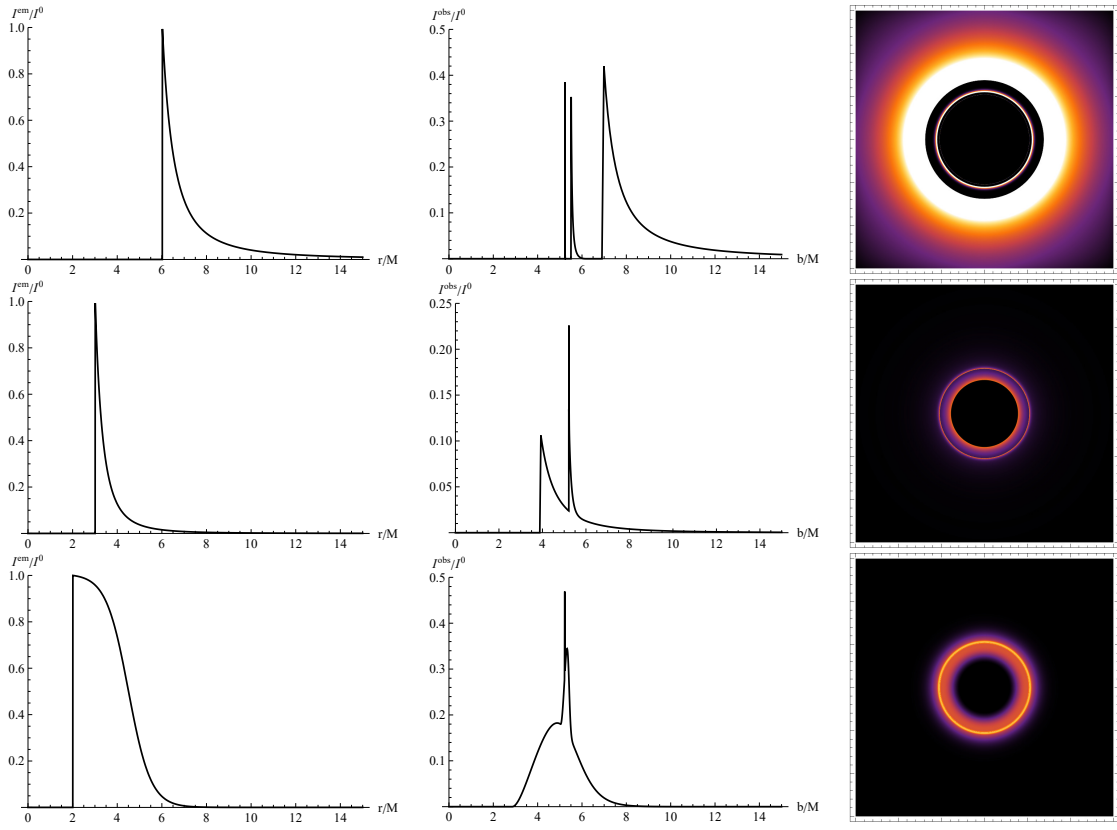


Figure 3: Emission specific intensity diagram (left), observation specific intensity diagram (middle) and halo diagram (right) of three emission models

In Model *I*, due to gravitational lensing in the observed intensity we clearly see the two isolated spikes representing the photon ring and lensing emissions, together with the more gradual decrease of the direct emission at larger impact parameter, neatly separated from each other. Therefore, the main contribution to the total

luminosity in the optical appearance is provided by the direct emission yielding a wide ring, while inner to it we find the lensing ring and in the innermost region the barely visible to naked eye is the photon ring. Therefore, we only calculate the transfer function to $m = 3$, when $m > 3$, the halo width can be ignored.

In Model *II*, the direct, lensed, and photon ring emissions are overlapped in the observed intensity in a wider range of impact parameters. The observed light intensity mainly has two peaks, the short but wide peak on the left is the direct emission peak, and the high but narrow peak on the right is obtained by the superposition of the peaks of the lensing ring and the photon ring.

In Model *III*, the direct observed region in impact parameter extends all the way down to the event horizon, increasing from there and getting again contributions at larger impact factors from the spike in the light ring first and in the lensing ring shortly after, before smoothly falling off to zero. The optical appearance in this case shows a narrow but somewhat brighter extended ring, made up of the contributions of the direct, lensing and photon ring emission, though as usual the latter can be safely ignored. This description of the optical appearances in these three models is completely consistent with the features obtained in similar images from the original description of the Schwarzschild black hole introduced in [15].

In addition, we calculated the light intensity diagram of Model *I* under different parameters. From Figure 4, we can see that the transformation trend is indeed like

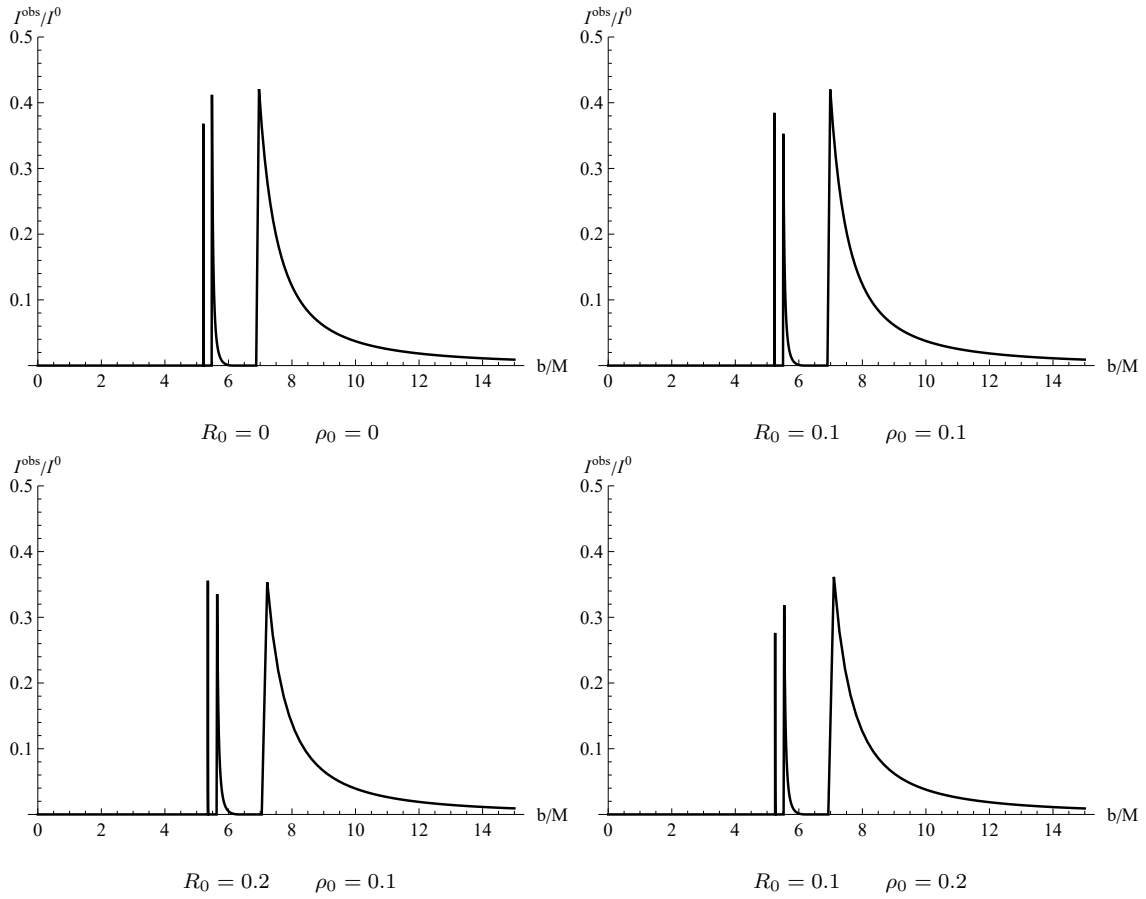


Figure 4: Observation specific intensity diagram of Model *I* under different parameters

what we analyzed in Section III. The halo radius increases with the increase of the CDM halo parameters, and the influence of R_0 is greater than that of ρ_0 . Moreover, due to energy conservation, the larger the CDM halo parameters, the smaller the peak of specific light intensity.

VI. CONCLUSION AND OUTLOOK

In this paper, we first calculate the null geodesic of Schwarzschild black hole in the CDM halo, and classify it according to its orbit deflection angle. From this, we analyze the relationship between the halo radius and the parameters of the CDM halo. Then we calculate the relationship between the light intensity emitted by the thin accretion disk and the observed light intensity of the viewer and the transfer function. Finally, we calculated three radiation models, analyzed their characteristics, and analyzed the relationship between the observed halo radius, intensity and the CDM halo parameters applicable to all radiation modes in the CDM halo, which is consistent with the previous analysis results.

Finally, we look forward to this paper. Firstly, we try to calculate the radiation of thin accretion disk in other dark matter models and black hole models. Secondly, it is proposed in [22] that a new shadow is found in the symmetrical thin shell wormhole connecting two different vacuum Schwarzschild spacetime. Similarly, in the case of the CDM halo, there should also be a new shadow in the symmetrical thin shell wormhole connecting two different Schwarzschild spacetime. Therefore, it is worth studying whether there is a new shadow when considering the influence of the CDM halo.

CONFLICTS OF INTEREST

The authors declare that there are no conflicts of interest regarding the publication of this paper.

REFERENCES

- [1] Albert Einstein. Die feldgleichungen der gravitation. *Sitzung der physikalisch-mathematischen Klasse*, 25:844–847, 1915.
- [2] A Einstein. Näherungsweise integration der feldgleichungen der gravitation, 22 jun 1916. 1916.
- [3] A Einstein. Kosmologische betrachtungen zur allgemeinen relativitätstheorie, 8 feb 1917. 1917.
- [4] Remo Ruffini and H Ohanian. Gravitation and spacetime, 1994.
- [5] Seven-Year Wilson Microwave Anisotropy Probe. Observations: Sky maps, systematic errors, and basic results. nasa. gov. Technical report, Retrieved 2010-12-02.
- [6] Sean M Carroll. *Dark Matter, Dark Energy: The Dark Side of the Universe. Parts 1 & 2*. Teaching Company, 2007.

- [7] Fritz Zwicky. Die rotverschiebung von extragalaktischen nebeln. *Helvetica physica acta*, 6:110–127, 1933.
- [8] PJE Peebles. Large scale background temperature and mass fluctuations due to scale invariant primeval perturbations, 1982.
- [9] John Michael Kovac, EM Leitch, Clement Pryke, JE Carlstrom, NW Halverson, and WL Holzapfel. Detection of polarization in the cosmic microwave background using dasi. *Nature*, 420(6917):772–787, 2002.
- [10] Peter AR Ade, N Aghanim, M Arnaud, Mark Ashdown, J Aumont, C Baccigalupi, AJ Banday, RB Barreiro, JG Bartlett, N Bartolo, et al. Planck 2015 results-xiii. cosmological parameters. *Astronomy & Astrophysics*, 594:A13, 2016.
- [11] Houjun Mo, Frank Van den Bosch, and Simon White. *Galaxy formation and evolution*. Cambridge University Press, 2010.
- [12] Zhaoyi Xu, Xian Hou, Xiaobo Gong, and Jiancheng Wang. Black hole space-time in dark matter halo. *Journal of Cosmology and Astroparticle Physics*, 2018(09):038, 2018.
- [13] NI Shakura. Critical luminosity for accretion and shell energy sources. *Soviet Astronomy*, 18:259, 1974.
- [14] RA Sunyaev. Accretion of matter onto black holes. In *Symposium-International Astronomical Union*, volume 64, pages 193–193. Cambridge University Press, 1974.

- [15] Samuel E Gralla, Daniel E Holz, and Robert M Wald. Black hole shadows, photon rings, and lensing rings. *Physical Review D*, 100(2):024018, 2019.
- [16] Samuel E Gralla. Measuring the shape of a black hole photon ring. *Physical Review D*, 102(4):044017, 2020.
- [17] Samuel E Gralla and Alexandru Lupsasca. Observable shape of black hole photon rings. *Physical Review D*, 102(12):124003, 2020.
- [18] Elizabeth Himwich, Michael D Johnson, Alexandru Lupsasca, and Andrew Strominger. Universal polarimetric signatures of the black hole photon ring. *Physical Review D*, 101(8):084020, 2020.
- [19] Xiao-Xiong Zeng and Hai-Qing Zhang. Influence of quintessence dark energy on the shadow of black hole. *The European Physical Journal C*, 80(11):1–14, 2020.
- [20] CA Chant. Notes and queries (telescopes and observatory equipment-the einstein shift of solar lines). *Journal of the Royal Astronomical Society of Canada*, 24:390, 1930.
- [21] George B Rybicki and Benjamin C Bromley. Emission line formation in a relativistic accretion disk. *arXiv preprint astro-ph/9711104*, 1997.
- [22] Xiaobao Wang, Peng-Cheng Li, Cheng-Yong Zhang, and Minyong Guo. Novel shadows from the asymmetric thin-shell wormhole. *Physics Letters B*, 811:135930, 2020.